The American Journal of Pathology, Vol. 172, No. 6, June 2008
Copyright © American Society for Investigative Pathology
DOI: 10.2353/ajpath.2008.071054

Tumorigenesis and Neoplastic Progression

Stat3 Promotes Metastatic Progression of Prostate Cancer

Junaid Abdulghani,* Lei Gu,* Ayush Dagvadorj,* Jacqueline Lutz,* Benjamin Leiby,† Gloria Bonuccelli,* Michael P. Lisanti,* Tobias Zellweger,‡ Kalle Alanen,§ Tuomas Mirtti,§ Tapio Visakorpi,¶ Lukas Bubendorf,‖ and Marja T. Nevalainen*

From the Department of Cancer Biology, Kimmel Cancer Center, and the Department of Pharmacology and Experimental Therapeutics,† Thomas Jefferson University, Philadelphia, Pennsylvania; the Department of Urology,‡ St. Clara Hospital, Basel, Switzerland; the Institute for Pathology,‖ University Hospital Basel, Basel, Switzerland; the Department of Pathology,§ Institute of Biomedicine, University of Turku, Turku, Finland; and the Institute of Medical Technology,¶ University of Tampere and Tampere University Hospital, Tampere, Finland*

There are currently no effective therapies for metastatic prostate cancer because the molecular mechanisms that underlie the metastatic spread of primary prostate cancer are unclear. Transcription factor Stat3 is constitutively active in malignant prostate epithelium, and its activation is associated with high histological grade and advanced cancer stage. In this work, we hypothesized that Stat3 stimulates metastatic progression of prostate cancer. We show that Stat3 is active in 77% of lymph node and 67% of bone metastases of clinical human prostate cancers. Importantly, adenoviral gene delivery of wild-type Stat3 (AdWTStat3) to DU145 human prostate cancer cells increased the number of lung metastases by 33-fold in an experimental metastasis assay compared with controls. Using various methods to inhibit Stat3, we demonstrated that Stat3 promotes human prostate cancer cell migration. Stat3 induced the formation of lamellipodia in both DU145 and PC-3 cells, further supporting the concept that Stat3 promotes a migratory phenotype of human prostate cancer cells. Moreover, Stat3 caused the rearrangement of cytoplasmic actin stress fibers and microtubules in both DU145 and PC-3 cells. Finally, inhibition of the Jak2 tyrosine kinase decreased both activation of Stat3 and prostate cancer cell motility. Collectively, these data indicate that transcription factor Stat3 is involved in metastatic behavior of human prostate cancer cells and may provide a therapeutic target to prevent metastatic spread of primary prostate cancer. ***(Am J Pathol 2008, 172:1717–1728; DOI: 10.2353/ajpath.2008.071054)***

Progression of prostate cancer to metastatic disease is one of the key problems in the clinical management of prostate cancer.[1] This is because there are currently no effective therapies for metastatic prostate cancer, and metastatic prostate cancer is the lethal form of the disease. Identification of the molecular changes that lead to formation of distant metastasis is critical for improvement of therapeutic interventions for metastatic prostate cancer and for development of strategies to prevent primary prostate cancer from metastasizing.

Transcription factor Stat3 has been implicated in the promotion of growth and progression of prostate cancer. Stat3, which is both a cytoplasmic signaling molecule and a nuclear transcription factor, belongs to the seven-member Stat gene family of transcription factors.[2] Stat3 becomes active by phosphorylation of a specific tyrosine residue in the carboxy-terminal domain by a tyrosine kinase (pY705).[3] Activation of Stat3 is supplemented by phosphorylation of a specific serine residue (S727).[4] After phosphorylation, Stat3 homodimerizes and translocates to the nucleus where it binds to specific Stat3 response elements of target gene promoters to regulate transcription.[3] Transcription factor Stat3 is constitutively active in clinical human prostate cancer,[5–9] and activation of Stat3 has been associated with advanced stage of prostate cancer.[5,9] Moreover, several reports implicate Stat3 in promotion of prostate cancer cell proliferation and inhibition of apoptosis.[5,10,11]

Supported by the National Institutes of Health (Cancer Center support grant CA56035-08 to the Kimmel Cancer Center) and the Department of Defense Prostate Cancer Research Program (Idea Development grant W81XWH-06-01-0076 to M.T.N.).

J.A. and L.G. contributed equally to this study.

Accepted for publication February 14, 2008.

Address reprint requests to Marja T. Nevalainen, M.D., Ph.D., Dept. of Cancer Biology, Kimmel Cancer Center, Thomas Jefferson University, 233 S. 10th St., BLSB 309, Philadelphia, PA 19107. E-mail: marja.nevalainen@jefferson.edu or m_nevalainen@mail.jci.tju.edu.

Recent studies have linked Stat3 to metastatic progression of several different cancer types. These include lung, skin, liver, ovarian, kidney, and colon cancer.[12–17] Contribution of Stat3 to metastatic progression of these cancers occurs through a variety of molecular mechanisms. Stat3 was associated with a migratory phenotype of lung cancer cells[12] while promoting angiogenesis of melanoma and hepatocellular cancer in animal tumor models.[13,14] In ovarian cancer, Stat3 was suggested to increase cell motility and invasion through effects on cell adhesion and cytoskeleton.[15] Moreover, a number of studies using mouse embryo fibroblasts as the model system established Stat3 as a component of RhoGTPase-signaling cascade and an effector of cell migration via regulation of actin cytoskeleton.[18–22] In addition, Stat3 was linked to cell migration via regulation of microtubules by interaction with stathmin protein.[23] In colon and renal cancer, active Stat3 expression was associated with tumor invasion and poor clinical outcome in patients.[16,17] Based on these findings, we formed the hypothesis that Stat3 contributes to the progression of prostate cancer to advanced disease by promoting metastatic spread of human prostate cancer cells.

Here, we show that Stat3 induces metastatic behavior of human prostate cancer cells *in vitro* and *in vivo*. First, using activation-specific Stat3 antibody we show that phosphorylated Stat3 localized in the nucleus and is activated in 77% of lymph node and 67% of bone metastases of clinical human prostate cancer. Gene delivery of wild-type Stat3 by adenovirus (AdWTStat3) to DU145 and PC-3 cells promoted migration of the cells as shown by wound filling and Boyden chamber assays. Moreover, Stat3 promoted formation of lamellipodia in both DU145 and PC-3 cells, which was accompanied by a phenotypic change in the cytoplasmic arrangement of actin stress fibers and microtubules. Importantly, Stat3 induced a 33-fold increase in colonization of DU145 cells to the lungs of nude athymic mice. Stat3 activation in human prostate cancer cells did not involve RhoGTPases but was rather mediated by Jak2 tyrosine kinase. In summary, Stat3 promotes metastatic behavior of human prostate cancer cells and may provide a therapeutic target protein to prevent metastatic progression of primary human prostate cancer.

Materials and Methods

Clinical Human Prostate Cancer Specimens and Prostate Cancer Metastases

The recurrent human prostate cancer specimens (n = 188) were obtained from the Tampere University Hospital, Tampere, Finland (n = 76)[24] and from the Institute for Pathology, University of Basel, Basel, Switzerland (n = 112).[25] All samples were transurethral resections from local recurrences. Of the 188 patients, 121 had received androgen ablation therapy (orchiectomy, n = 76; luteinizing hormone-releasing hormone, n = 19; estrogen, n = 1; anti-androgen, n = 2; orchiectomy + estrogen, n = 2; maximal androgen blockade, n = 21), whereas the rest (n = 67) had received no hormonal treatment. Paraffin-embedded prostate cancer metastases were obtained from the Turku University Hospital, Turku, Finland (n = 95) (lymph node, n = 44; to bone, n = 1; to other organs, n = 50) and from Georgetown University, Washington, DC (lymph node, n = 22; to bone, n = 14) (approved by the Thomas Jefferson University Institutional Review Board).

Adenoviral Gene Delivery

Adenoviruses carrying human wild-type Stat3 (AdWTStat3), transcriptionally inactive Stat3 (AdDNStat3) (C-terminally truncated at amino acid 715), wild-type Jak2 (AdWtJak2), and a kinase-domain deleted dominant-negative Jak2 (AdDNJak2) were a gift from Dr. Hallgeir Rui at Thomas Jefferson University.[26] Viral stocks were expanded in large-scale cultures, purified by double cesium chloride gradient centrifugation, and titered side-by-side by a standard plaque assay method in QBI-HEK-293A cells (Qbiogene, Carlsbad, CA) per the manufacturer's instructions. For adenoviral gene delivery, DU145 and PC-3 cells were infected with AdDNStat3, AdWTStat3, AdWTJak2, or AdDNJak2 at multiplicity of infection (m.o.i.) of 10 for 90 minutes, after which RPMI 1640 containing 10% fetal bovine serum (FBS) was added.

Immunostaining of Paraffin-Embedded Tissue Sections

Slides containing deparaffinized formalin-fixed prostate cancer sections were microwaved in a pressure-cooker with antigen retrieval solution AR-10 (BioGenex Laboratories, San Ramon, CA). Endogenous peroxidase activity was blocked by 0.3% hydrogen peroxide, and nonspecific binding of immunoglobulin was minimized by preincubation in 10% normal goat serum for 2 hours at room temperature. Anti-phosphotyrosine-Stat3 (Y705) polyclonal antibody (pAb) (Cell Signaling, Danvers, MA) was used at a concentration of 1:100. Antigen-antibody complexes were detected using a biotinylated goat anti-rabbit secondary antibody (BioGenex Laboratories) followed by streptavidin-horseradish-peroxidase complex using 3,3(prime)-diaminobenzidine as chromogen and Mayer hematoxylin as counterstain.

Scoring of Levels of Active Stat3 in Metastatic and Recurrent Clinical Human Prostate Cancers

Individual prostate tumor samples were scored (M.T.N. and J.A.) for active nuclear Stat3 levels on a scale from 0 to 3, where 0 is undetectable and 1 represented positive immunostaining.

Solubilization of Proteins, Immunoprecipitation, and Immunoblotting

For immunoprecipitation, DU145, LNCaP, PC-3, and CWR22*Rv*1 prostate cancer cells were lysed in lysis

buffer [10 mmol/L Tris-HCl (pH 7.6), 5 mmol/L ethylenediaminetetraacetic acid, 50 mmol/L NaCl, 30 mmol/L sodium pyrophosphate, 50 mmol/L sodium fluoride, 1 mmol/L sodium orthovanadate, 1% Triton X-100, 1 mmol/L phenylmethyl sulfonyl fluoride, 5 μg/ml aprotinin, 1 μg/ml pepstatin A, and 2 μg/ml leupeptin]. The cell lysates were immunoprecipitated for 2 hours with anti-Stat3 pAb (a gift from Dr. Robert Kirken, University of Texas, El Paso). Antibodies were captured by incubation for 2 hours with protein A-Sepharose beads (Pharmacia Biotech, Piscataway, NJ). The primary antibodies were used at the following concentrations: anti-phosphotyrosine Stat3 pAb (Y705, 1:1000; Cell Signaling), anti-phosphoserine Stat3 pAb (1:1000, Cell Signaling), anti-Stat3 mAb (1:1000; Santa Cruz Biotechnology, Santa Cruz, CA), anti-Jak2 pAb (1:1000; Upstate Biotechnology, Lake Placid, NY), anti-actin pAb (1:3000; Sigma, St. Louis, MO) and detected by horseradish peroxidase-conjugated secondary antibodies in conjunction with enhanced chemiluminescence substrate mixture (Amersham, Piscataway, NJ) and exposed to film. RhoA inhibitors (555550 and Y27632) and a Rac1 inhibitor (553502) were purchased from Calbiochem (San Diego, CA).

Wound Filling Assay

DU145 (1.5×10^6 cells/well) or PC-3 (1.25×10^6 cells/well) cells were mock-infected or infected with AdWTStat3, AdDNStat3, AdWTJak2, or AdDNJak2 at a m.o.i. of 10. Identical scratches were made in parallel wells 24 hours after infection using a 1000-μl plastic pipette tip. The cells were fixed by 0.5% crystal violet solution (Sigma) at 0, 24, 48, and 72 hours. The size of wound was measured and the percentage of the cells that had migrated was calculated.

Cell Motility Assay

DU145 and PC-3 cells were mock-infected or infected with AdLacZ, AdWTStat3, AdDNStat3, AdWTJak2, or AdDNJak2 at a m.o.i. of 10. Cells were harvested 24 hours after infection and single-cell suspension of 2.5×10^4 cells was added to the upper chamber of a motility chamber system (8.0 μm pore size; BD BioSciences, San Jose, CA) (modified Boyden chamber assay). FBS (5%) in RPMI media was used as chemoattractant in the lower chamber. The cells were incubated for 24 hours, and the cells that traversed the membrane pores to the lower membrane were fixed, stained with the Diff Quik staining kit (Dade Behring Inc., Newark, DE) and counted in four different quadrants. Each experiment was done in triplicate and error bars represent the mean ± SE.

siRNA Transfections

Human Stat3 and control siRNA were from Dharmacon (Lafayette, CO). DU145 cells at 40 to 50% confluence were transfected with Stat3 or scrambled control siRNA (100 pmol/well of a 3-cm well) using Lipofectamine2000 (Invitrogen, Carlsbad, CA) according to the manufacturer's instructions. After 24, 48, or 72 hours, the cells were harvested for Western blotting, cell viability assays, or microtubule immunocytochemistry.

Clustering Assay

DU145 and PC-3 cells were infected with AdWTStat3 or AdDNStat3 at a m.o.i. of 10. Twenty-four hours after adenoviral infection, the cells were seeded on Matrigel (total protein, 8.5 mg/ml; endotoxin, 1.0 U/ml) (BD Biosciences) that was spread on glass coverslips. After incubation for 96 hours, the cells were observed for morphological alterations and photographed (Nikon Stereoscope, Chuoku, Japan).

Quantification of the Volume of Lamellipodia

Photographs of wound margins from wound filling assay of DU145 cells were analyzed for lamellipodia. The areas of lamellipodia along the wound margins were measured using the Metamorph program (Molecular Devices, Sunnyvale, CA). The surface areas of lamellipodia were calculated per cell and plotted on a graph.

Immunofluorescence Cytochemistry of Actin and Tubulin

DU145 (3×10^4 cells) and PC-3 (1.5×10^4) cells grown on cover glasses were mock-infected or infected with AdWTStat3, AdDNStat3, AdWTJak2, or AdDNJak2 at a m.o.i. of 10. Forty-eight hours after adenoviral expression of Stat3 and Jak2 proteins, the cells were fixed with 4% paraformaldehyde in phosphate-buffered saline for 15 minutes followed by permeabilization with 0.1% Triton X-100 in 4% paraformaldehyde in phosphate-buffered saline for 15 minutes. The cells were incubated with rhodamine-conjugated phalloidin (Invitrogen, Eugene, OR) for 1 hour. For immunofluorescence cytochemistry of tubulin, 4% paraformaldehyde and 0.1% Triton X-100 were made in PHEM buffer (60 mM PIPES, 27.5 mM HEPES, 10 mM EGTA, 8 mM $MgSO_4$, pH 7), and the cells were stained with an antibody against tubulin (clone TU-01; Invitrogen) diluted (1:100) in blocking buffer, which was detected with fluorescein isothiocyanate (FITC)-conjugated secondary antibody (Invitrogen). The nuclei were stained with mounting media containing 4,6-diamidino-2-phenylindole (Vector Laboratories, Burlingame, CA) and examined under a LSM510 META confocal laser scanning microscope with an ×63 objective (Zeiss, Thornwood, NY).

Tail-Vein Injections of Human Prostate Cancer Cells

Castrated male athymic mice were purchased from Taconic (Germantown, NY) and cared for according to the institutional guidelines. DU145 cells were infected with a m.o.i. of 10 of AdLacZ, AdWTStat3, and AdDNStat3. After 24 hours, 1×10^6 cells were suspended in 0.2 ml of

phosphate-buffered saline and injected into the lateral tail vein using a 27-gauge needle. The mice were sacrificed 8 weeks after inoculation, and the lungs were perfused with 1.5 ml of 15% India ink dye in 3.7% formalin. Lungs were then removed, rinsed in water for 15 seconds, and bleached in Fekete's solution (70% ethanol, 3.7% formaldehyde, 0.75 mol/L glacial acetic acid). Lung surfaces were photographed and scored.

Statistical Analysis

Differences in groups with respect to number of migrated cells and wound size were assessed using two-sample *t*-tests or analysis of variance as appropriate. Pair-wise comparisons were performed if the overall analysis of variance test for differences in means was significant. *P* values for these comparisons were adjusted using Tukey's procedure.

Results

Stat3 Is Activated in Clinical Prostate Cancer Metastasis and in Recurrent Prostate Cancer

As the first step to test the hypothesis that Stat3 promotes metastatic behavior of human prostate cancer cells, we determined how frequently Stat3 is activated in clinical prostate cancer metastases (n = 131) and recurrent human prostate cancers (n = 181). Stat3 activation was analyzed by immunohistochemical detection of paraffin-embedded tissue sections. In addition to active Stat3 immunostaining, prostate cancer metastases sections were immunostained for PSA to verify the location of prostate cancer cells within the metastases-containing tissues. Parallel sections were stained with normal rabbit serum as a negative control (data not shown). Representative prostate cancer metastases to bone and lymph nodes with positive immunoreaction for active Stat3 and PSA are presented in Figure 1, A and B.

A positive immunoreaction for active Stat3 was detected in 64% (84 of 131) of prostate cancer metastases (Table 1). In prostate cancer metastases to regional lymph nodes, an intense immunoreaction for active Stat3 was detected in 77% (51 of 66) of the specimens, whereas Stat3 was activated in 67% (10 of 15) of the bone metastases. Moreover, Stat3 was active in 56% (28 of 50) of prostate cancer metastases to distant organs other than bone. To further investigate Stat3 activation in advanced prostate cancer, we assessed Stat3 activation in recurrent human prostate tumors. Significant activation of Stat3 was detected in 86% (162 of 188) of recurrent human prostate cancer specimens (Table 1). Of these 188 patients, 121 had been treated with androgen deprivation before the recurrence occurred (see Materials and Methods section). Stat3 was constitutively active in 96 of the 121 recurrent prostate cancers (79%) treated with hormone therapy (Table 1). In summary, our results indicate that Stat3 is constitutively active in the majority of distant prostate cancer metastases and in recurrent hormone-refractory prostate cancer.

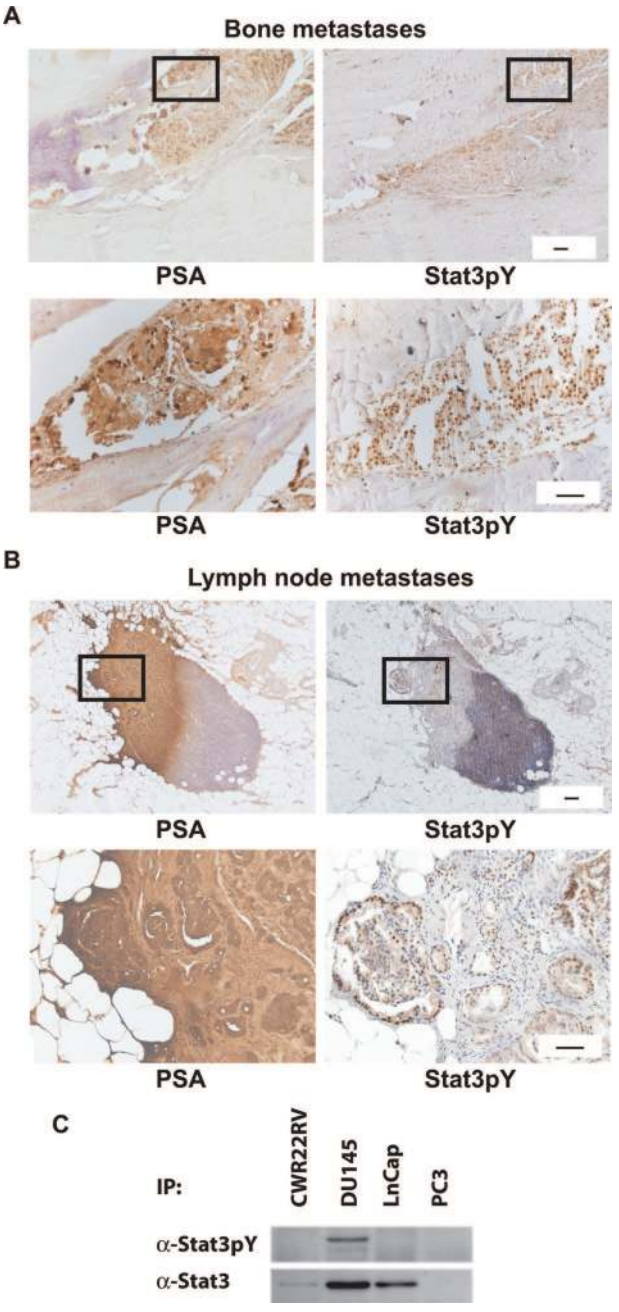

Figure 1. Activation of Stat3 in human prostate cancer metastases to lymph nodes and to bone. Activation of Stat3 in prostate cancer metastases was analyzed by immunohistochemical staining using a polyclonal anti-Stat3pY antibody in paraffin-embedded tissue sections. 3,3′-Diaminobenzidine (3,3′-DAB) was used as a chromogen and Mayer hematoxylin as a counterstain. Biotin-streptavidin-amplified peroxidase-antiperoxidase immunodetection shows intense positive reactions for active Stat3 in the nuclei of prostate cancer cells metastasized to bone (**A**) and lymph nodes (**B**) (**right**). Parallel sections were immunostained for prostate-specific antigen (PSA) to verify the location of prostate cancer cells in the metastases tissues (**left**). **C:** Stat3 protein is expressed in CWR22*Rv*1, DU145, and LNCaP human prostate cancer cells, whereas PC-3 cells are negative for Stat3. Stat3 is constitutively active only in DU145 cells. Immunoprecipitated Stat3 was blotted with anti-phosphoTyrStat3 (anti-Stat3pY) pAb and parallel samples were immunoblotted with anti-Stat3 mAb as indicated. Scale bars = 50 μm.

Table 1. Stat3 Activation in Prostate Cancer Metastasis and in Recurrent Hormone-Refractory Prostate Cancers

	Number of patients	%
Prostate cancer metastasis	131	100
Stat3 activation, negative	47	36
Stat3 activation, positive	84	64
Prostate cancer to regional lymph nodes	66	100
Stat3 activation, negative	15	23
Stat3 activation, positive	51	77
Prostate cancer to bone	15	100
Stat3 activation, negative	5	33
Stat3 activation, positive	10	67
Prostate cancer to other organs	50	100
Stat3 activation, negative	22	44
Stat3 activation, positive	28	56
Recurrent prostate cancers	188	100
Stat3 activation, negative	26	14
Stat3 activation, positive	162	86
Recurrent prostate cancers treated with hormone therapy	121	100
Stat3 activation, negative	25	21
Stat3 activation, positive	96	79

Stat3 Promotes Motility of Human Prostate Cancer Cells

Given that Stat3 is constitutively active in the majority of clinical human prostate cancer metastases (Table 1), we aimed to determine whether Stat3 is involved in the regulation of metastatic behavior of prostate cancer cells *in vitro*. The metastatic process is a sequential cascade of multiple cellular events involving invasion of the cells into extracellular matrix, migration of the cells, changes in homo- and heterotypic adhesion, as well as changes in angiogenesis. We chose first to focus on establishing the effects of Stat3 on prostate cancer cell migration because previous studies have suggested that Stat3 proteins may affect cell motility in other cancer types.[12,15,19,23] DU145 and PC-3 cells were selected as the experimental models because both cell lines are androgen-independent with high metastatic potential in *in vivo* studies.[27–31] Moreover, DU145 cells express high levels of active Stat3, whereas PC-3 cells do not endogenously express Stat3 (Figure 1C) because of a deletion of the Stat3 gene.[32]

The migration of DU145 cells was increased by 2.8-fold in cells infected with AdWTStat3 (m.o.i. = 10), compared to cells infected with transcriptionally inactive Stat3 (AdDNStat3) (m.o.i. = 10) ($P < 0.0001$) as determined by wound filling assay 48 hours after adenoviral exposure (Figure 2A, a and b). Endogenous Stat3 in AdLacZ-infected cells promoted migration by 1.6-fold compared to the AdDNStat3-infected group ($P < 0.0001$), which is probably attributable to a dominant-negative effect of transcriptionally inactive Stat3 on the endogenous Stat3. When the modified Boyden chamber assay was performed using 5% FBS as a chemoattractant, the motility of DU145 cells was increased by 1.7-fold 48 hours after the adenoviral gene delivery of AdWTStat3 compared to cells expressing DNStat3 ($P < 0.0001$) (Figure 2Ac). When Stat3 was introduced by adenoviral gene delivery to PC-3 cells, which do not endogenously express Stat3, migration of PC-3 cells was increased by fivefold in the wound filling assay at 24 hours compared to the control group (AdLacZ) ($P < 0.0001$) (Figure 2B, a and b). In modified Boyden chamber assays, migration of PC-3 cells expressing WTStat3 was increased by 1.7-fold compared to the control group (AdLacZ) ($P < 0.0001$) 24 hours after adenoviral exposure (Figure 2Bc). As evident from Figure 2, A and B, DU145 cells migrated in sheet-like structures, whereas PC-3 cells migrated as individual cells. The efficiency of adenoviral gene delivery of Stat3 proteins to PC-3 cells is demonstrated by Western blotting in Figure 2C. In summary, these data provide support for the concept that Stat3 induces motility of DU145 and PC-3 human prostate cancer cells *in vitro*.

Stat3 Decreases Homotypic Cell Clustering and Induces Lamellipodia Formation

To investigate the role of Stat3 in the invasive capacity of human prostate cancer cells *in vitro*, we examined the effects of Stat3 on homotypic cluster formation of DU145 cells cultured on Matrigel, a collagen-rich extracellular matrix that provides a more physiological growth environment than plastic. DU145 cells (Figure 3A) were infected with adenovirus expressing WTStat3 or DNStat3 (m.o.i. = 10), and cultured on Matrigel for 4 days. In the control groups (mock, AdDNStat3), DU145 cells formed large cell clusters within 96 hours as revealed by phase contrast stereomicroscopy (Figure 3A). In contrast, the cell clustering was essentially eliminated in cells overexpressing WTStat3, and the cells were instead highly scattered (Figure 3A). These data provided evidence that Stat3 disrupts homotypic cluster formation of DU145 cells, suggestive of increased migration and invasive potential.

Because overexpression of Stat3 in DU145 and PC-3 cells was associated with increased migration of the cells, we investigated whether Stat3 expression was associated with morphological changes characteristic to motile cells (Figure 3B). Specifically, it is known that the protrusion of the cell membrane is fundamental to cell shape changes related to cell migration. The leading edge drives the membrane protrusion and is dominated by thin actin-rich structures called lamellipodia. In the next set of experiments, DU145 and PC-3 cells were infected with adenovirus expressing WTStat3 or DNStat3 (m.o.i. = 10), and plated on wells coated with Matrigel. The cell morphology was observed at 24, 48, and 72 hours. DU145 and PC-3 cells infected with AdWTStat3 formed large lamellipodia at 48 and 24 hours, respectively (Figure 3B, a and b). In contrast, DU145 and PC-3 cells expressing DNStat3 or mock-infected cells formed large clusters without visible cell membrane protrusions (Figure 3B, a and b). We also analyzed and quantitated the surface area of lamellipodia in the wound filling assays of DU145 cells using a Metamorph imaging system

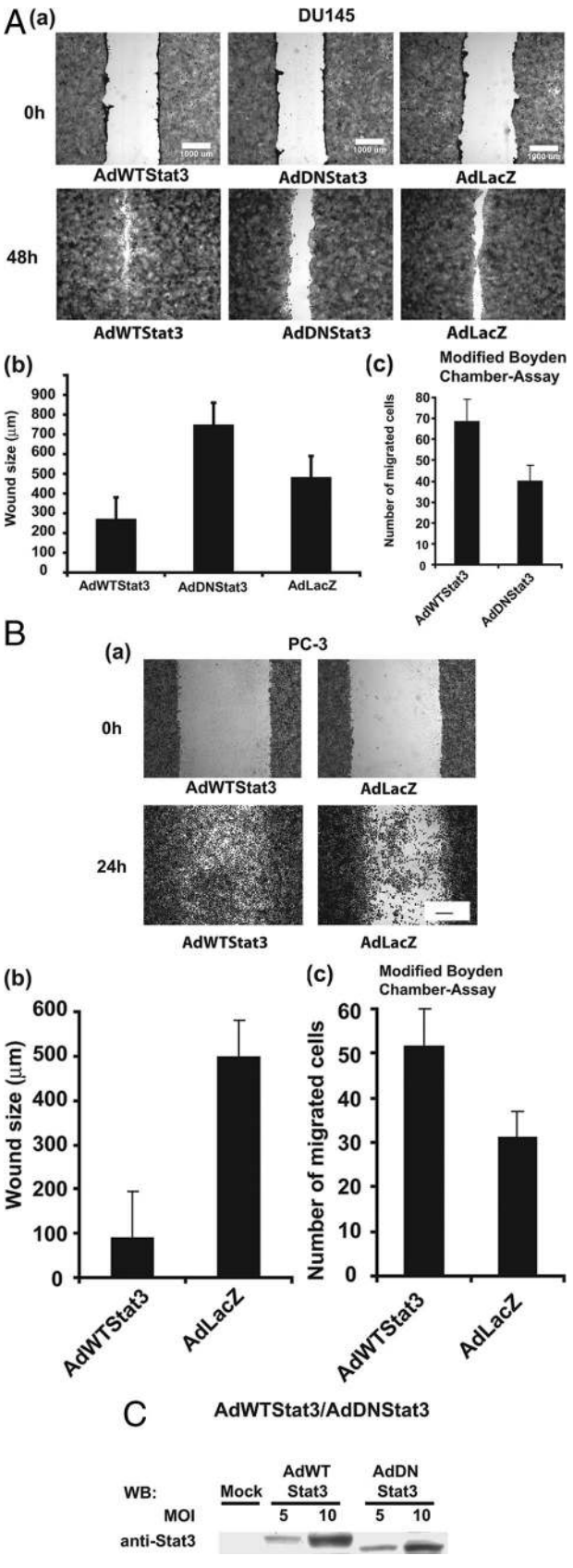

in the stereomicroscope. The volume of lamellipodia in DU145 cells infected with adenovirus expressing WTStat3 was increased by almost twofold compared to DU145 cells expressing DNStat3 (Figure 3B, c and d). In parallel experiments, we tested whether the migratory phenotype induced by Stat3 involved changes in E- or P-cadherin expression, which all yielded negative results (data not shown). Collectively, these results show that Stat3 induces lamellipodia formation in DU145 and PC-3 human prostate cancer cells.

Stat3 Induces Experimental Metastases of DU145 Cells

Because Stat3 induced migration of both DU145 and PC-3 cells *in vitro*, and because Stat3 is constitutively active in the majority of clinical human prostate cancer metastases, we next tested whether Stat3 will affect the *in vivo* metastasis process of human prostate cancer cells. We performed experimental metastases assay by infecting DU145 cells with adenovirus expressing WTStat3, DNStat3, or LacZ at a m.o.i. of 10. Twenty-four hours after the adenoviral gene delivery, we injected DU145 cells in athymic nude mice through the tail veins (1×10^6 cells per mouse). The lungs were harvested after 8 weeks and stained with India ink, bleached with Fekete's solution, and scored for surface lung metastases. As demonstrated in Figure 3C, the number of metastases in mice injected with DU145 cells infected with AdWTStat3 was increased by ~33-fold when compared to mice injected with DU145 cells that had been infected with either AdLacZ or AdDNStat3. Quantitatively, injection of AdWTStat3-infected DU145 cells resulted in an average of 232 (SEM = 53.3) metastases per lung, as compared with 7 per lung using DU145 cells infected with AdLacZ (SEM = 3.0) or AdDNStat3 (SEM = 4.4). As shown visually in Figure 3C (bottom), overexpression of Stat3 promotes experimental metastasis of human prostate cancer cells in nude mice with a number of white metastasis nodules in the lungs. This is the first demonstration that transcription factor Stat3 increases the intrinsic ability of prostate cancer cells to metastasize *in vivo*.

Figure 2. Stat3 promotes motility of prostate cancer cells. DU145 (**A**) and PC-3 cells (**B**) were infected with wild-type Stat3 adenovirus (AdWTStat3), dominant-negative Stat3 adenovirus (AdDNStat3), or adenovirus expressing β-galactosidase (AdLacZ) at m.o.i. of 10, as indicated. Identical scratches were made in parallel wells ($n = 8$) using a 1000-μl pipette tip 24 hours after the adenoviral infection. The cells were fixed with 0.5% crystal violet at 0 hours, 24 hours, 48 hours, and 72 hours. The wells were photographed (Nikon stereoscope), (**a**) and wound size measured (**b**). The peak differences between the treatment groups were observed at 48 hours and at 24 hours for DU145 (**A**) and PC-3 (**B**) cells, respectively, after the scratches were made. The mean values of four independent experiments each with two parallel wells per treatment (total, $n = 8$ per group) are presented and SD values are indicated. For modified Boyden chamber assays, DU145 and PC-3 cells were exposed to infection with adenovirus carrying either DNStat3 or WTStat3 at a m.o.i. of 10 for 90 minutes. Motility of DU145 (**A**) and PC-3 (**B**) cells through uncoated filters into the lower chamber of the microchemotaxis chambers filled with media containing 5% FBS was measured after 24 hours (**c**). Migrated cells were fixed, stained, and counted using phase contrast microscope in triplicate filters in three individual experiments (mean ± SD). **C:** Dose-dependent expression of WTStat3 or DNStat3 in PC-3 cells was detected by immunoblotting of the whole-cell lysates with anti-Stat3 pAb 24 hours after adenoviral gene transfer (m.o.i., 5 and 10). Scale bars = 1000 μm.

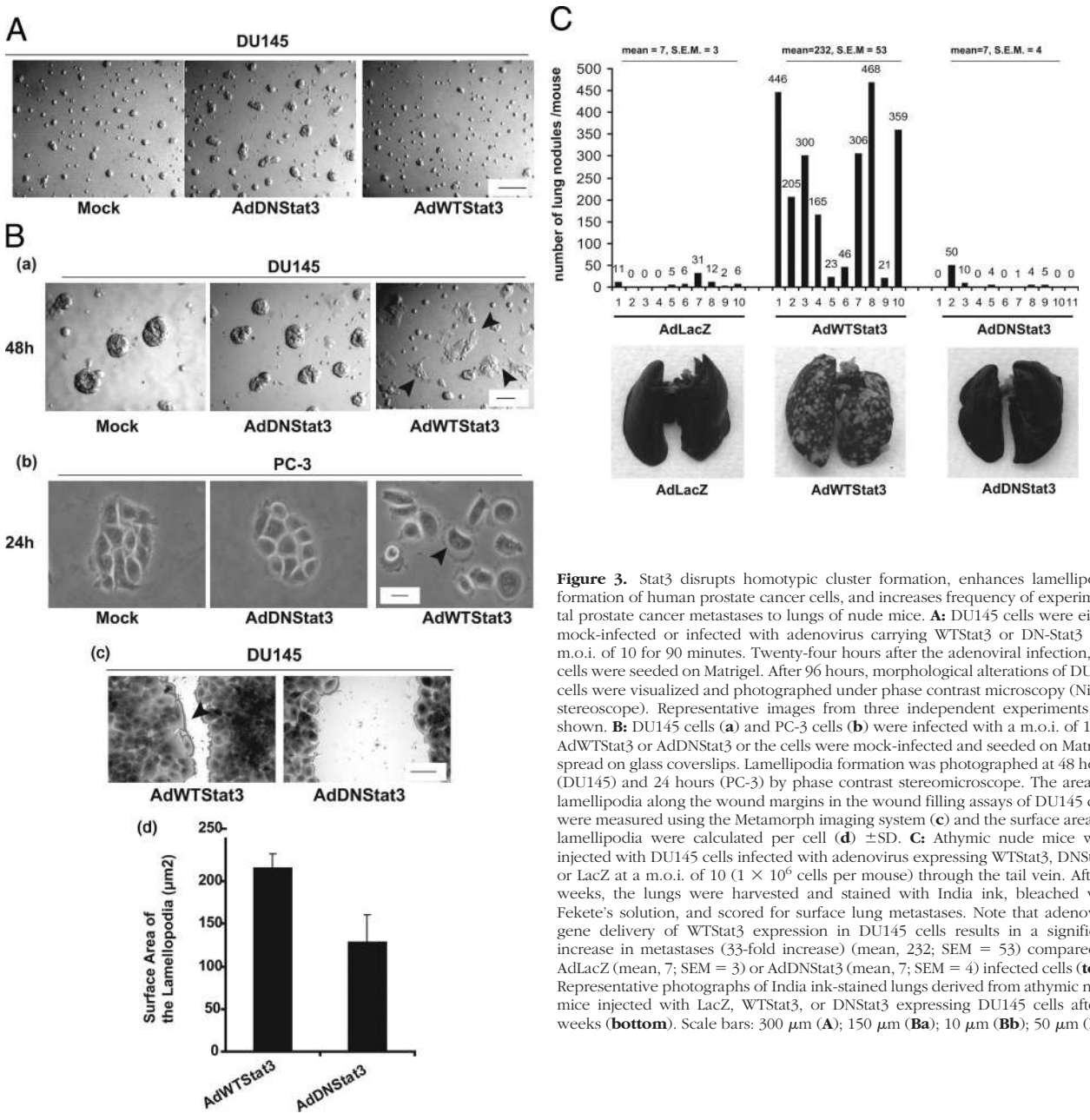

Figure 3. Stat3 disrupts homotypic cluster formation, enhances lamellipodia formation of human prostate cancer cells, and increases frequency of experimental prostate cancer metastases to lungs of nude mice. **A:** DU145 cells were either mock-infected or infected with adenovirus carrying WTStat3 or DN-Stat3 at a m.o.i. of 10 for 90 minutes. Twenty-four hours after the adenoviral infection, the cells were seeded on Matrigel. After 96 hours, morphological alterations of DU145 cells were visualized and photographed under phase contrast microscopy (Nikon stereoscope). Representative images from three independent experiments are shown. **B:** DU145 cells (**a**) and PC-3 cells (**b**) were infected with a m.o.i. of 10 of AdWTStat3 or AdDNStat3 or the cells were mock-infected and seeded on Matrigel spread on glass coverslips. Lamellipodia formation was photographed at 48 hours (DU145) and 24 hours (PC-3) by phase contrast stereomicroscope. The areas of lamellipodia along the wound margins in the wound filling assays of DU145 cells were measured using the Metamorph imaging system (**c**) and the surface areas of lamellipodia were calculated per cell (**d**) ±SD. **C:** Athymic nude mice were injected with DU145 cells infected with adenovirus expressing WTStat3, DNStat3, or LacZ at a m.o.i. of 10 (1×10^6 cells per mouse) through the tail vein. After 8 weeks, the lungs were harvested and stained with India ink, bleached with Fekete's solution, and scored for surface lung metastases. Note that adenoviral gene delivery of WTStat3 expression in DU145 cells results in a significant increase in metastases (33-fold increase) (mean, 232; SEM = 53) compared to AdLacZ (mean, 7; SEM = 3) or AdDNStat3 (mean, 7; SEM = 4) infected cells (**top**). Representative photographs of India ink-stained lungs derived from athymic nude mice injected with LacZ, WTStat3, or DNStat3 expressing DU145 cells after 8 weeks (**bottom**). Scale bars: 300 μm (**A**); 150 μm (**Ba**); 10 μm (**Bb**); 50 μm (**Bc**).

Stat3 Induces Polarization of Actin Cytoskeleton and the Microtubule Network of Prostate Cancer Cells

Because Stat3 promoted experimental metastases of human prostate cancer cells *in vivo*, we next focused our study on the molecular changes underlying Stat3-induced cell migration. Reorganization of the actin cytoskeleton and the microtubule network are the primary mechanisms of cell motility and essential for cell migration. Specifically, actin is organized in parallel bundles forming filopodia or a dense meshwork that forms ruffling lamellipodia. This reorganization of the actin cytoskeleton promotes protrusion of the leading edge of the cell.[33,34] In addition, filamentous actin forms contractile stress fibers in migrating cells and is responsible for the contraction of the cell body and retraction of the trailing edge. Because Stat3 induced lamellipodia formation in both DU145 and PC-3 cells, we examined whether Stat3 affects polymerization and organization of the actin cytoskeleton in prostate cancer cells. WTStat3 or DNStat3 were delivered to DU145 cells and PC-3 cells using adenovirus at a m.o.i. of 10 and mock-infected cells served as an additional control. Forty-eight hours after adenoviral expression of Stat3 proteins, the cells were fixed and immunostained for actin using FITC-conjugated secondary antibodies. In both DU145 and PC-3 cells, adenoviral expression of WTStat3 induced extensive polarization of the actin cytoskeleton (Figure 4A). Formation of actin bundles on the cell membrane extending to filopodia was

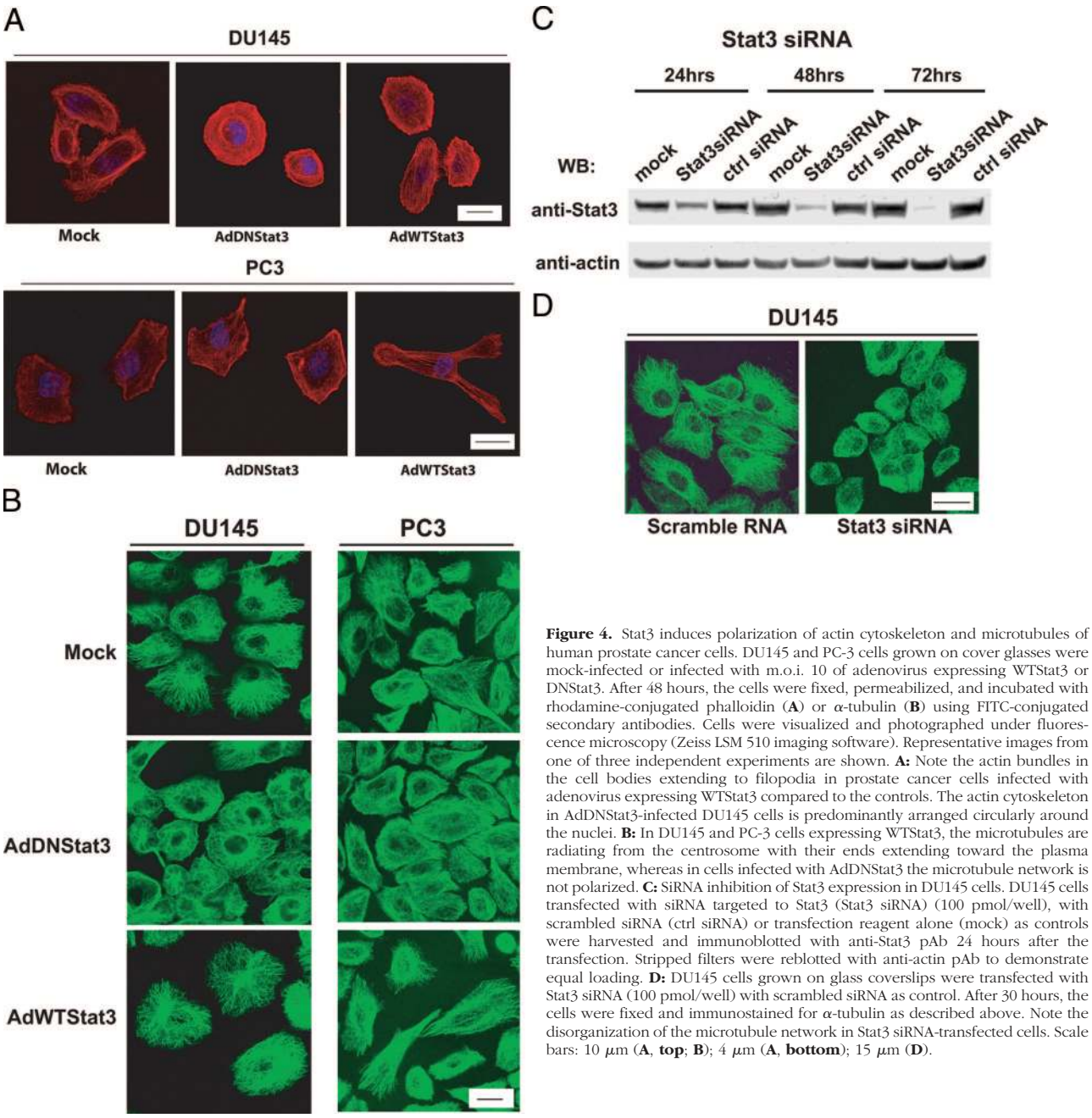

Figure 4. Stat3 induces polarization of actin cytoskeleton and microtubules of human prostate cancer cells. DU145 and PC-3 cells grown on cover glasses were mock-infected or infected with m.o.i. 10 of adenovirus expressing WTStat3 or DNStat3. After 48 hours, the cells were fixed, permeabilized, and incubated with rhodamine-conjugated phalloidin (**A**) or α-tubulin (**B**) using FITC-conjugated secondary antibodies. Cells were visualized and photographed under fluorescence microscopy (Zeiss LSM 510 imaging software). Representative images from one of three independent experiments are shown. **A:** Note the actin bundles in the cell bodies extending to filopodia in prostate cancer cells infected with adenovirus expressing WTStat3 compared to the controls. The actin cytoskeleton in AdDNStat3-infected DU145 cells is predominantly arranged circularly around the nuclei. **B:** In DU145 and PC-3 cells expressing WTStat3, the microtubules are radiating from the centrosome with their ends extending toward the plasma membrane, whereas in cells infected with AdDNStat3 the microtubule network is not polarized. **C:** SiRNA inhibition of Stat3 expression in DU145 cells. DU145 cells transfected with siRNA targeted to Stat3 (Stat3 siRNA) (100 pmol/well), with scrambled siRNA (ctrl siRNA) or transfection reagent alone (mock) as controls were harvested and immunoblotted with anti-Stat3 pAb 24 hours after the transfection. Stripped filters were reblotted with anti-actin pAb to demonstrate equal loading. **D:** DU145 cells grown on glass coverslips were transfected with Stat3 siRNA (100 pmol/well) with scrambled siRNA as control. After 30 hours, the cells were fixed and immunostained for α-tubulin as described above. Note the disorganization of the microtubule network in Stat3 siRNA-transfected cells. Scale bars: 10 μm (**A**, **top**; **B**); 4 μm (**A**, **bottom**); 15 μm (**D**).

evident, as well as formation of actin stress fibers in the cell body. In contrast, when DU145 cells were infected with adenovirus expressing DNStat3, the actin cytoskeleton was organized predominantly in an oval shape, reflecting a dominant-negative effect of AdDNStat3 on the endogenous Stat3 present in DU145 cells. The actin cytoskeleton was formed into a disorganized network in mock-infected DU145 and PC-3 cells as well as in AdDNStat3-infected PC-3 cells (Figure 4A).

Although the actin cytoskeleton provides protrusive and contractile forces, microtubules are important for the intrinsic cell polarization and directional cell migration. Specifically, microtubules are thought to provide a network that allows organelle and protein movement throughout the cell and are linked to actin polymers directly or through intermediate proteins or signaling molecules.[23,33,34] Our finding that Stat3 regulates the actin cytoskeleton organization led us to ask whether microtubule polarization is also affected by Stat3 in prostate cancer cells. Parallel wells of DU145 and PC-3 cells, immunostained for actin, were stained for the presence of α-tubulin using FITC-conjugated secondary antibodies (Figure 4B). Introduction of WTStat3 to DU145 or PC-3 cells by adenoviral gene delivery (m.o.i. = 10) resulted in polarization of the microtubules outwards from the centrosomes forming a dense meshwork toward the plasma membrane. In contrast, the microtubule network in DU145 cells expressing DNStat3 was disrupted, which is

characteristic to nonmigratory cells (Figure 4B). In mock-infected DU145 cells, endogenous Stat3 caused microtubule protrusion toward the plasma membrane, although to clearly a lesser extent when compared to AdWTStat3-infected cells. As expected, the microtubule cytoskeleton of mock-infected PC-3 cells resembled AdDNStat3-infected PC-3 cells exhibiting a network characteristic to nonmigratory cells because Stat3 gene is deleted in PC-3 cells. In addition to adenoviral expression of WTStat3 as an experimental model, we suppressed Stat3 expression by RNA interference in DU145 cells and examined the distribution of microtubules by immunostaining for α-tubulin. Efficiency of inhibition of Stat3 expression by Stat3 siRNA in DU145 cells is demonstrated by Western blotting (Figure 4C). In DU145 cells transfected with Stat3 siRNA, the microtubules were nonpolarized and wrapped around the nuclei (Figure 4D). On the contrary, in DU145 cells transfected with the control siRNA (Figure 4D), microtubules showed polarization and resembled the microtubule network organization in the mock-infected cells (Figure 4B). Taken together, these data supported the concept that Stat3 induces polarization of the actin cytoskeleton and the microtubule network in human prostate cancer cells.

Jak2, but Not RhoGTPases, Contributes to the Stat3-Induced Migration of Prostate Cancer Cells

As a next step, we aimed to identify the kinases involved in the activation of Stat3 and induction of prostate cancer cell migration. The major tyrosine kinases that are known to phosphorylate Stat3 are Jak1 and Jak2,[3] which leads to dimerization of Stat3 and translocation of the Stat3 dimer to the nucleus. However, in several different cell types, RhoGTPases are also known to mediate Ser-727 and Tyr-705 phosphorylation and nuclear translocation of Stat3.[18,19,35] Importantly, Rho family GTPases regulate the dynamics and organization of microtubules and the assembly of contractile actin in migratory cells.[33,36] To test whether RhoGTPases activate Stat3 in human prostate cancer cells, DU145 cells expressing constitutively active Stat3 were treated with increasing concentrations of pharmacological RhoA inhibitors (555550 and Y27632) and a Rac1 inhibitor (553502) for 24, 48, and 72 hours (Figure 5A). Western blotting of the cell lysates for tyrosine or serine phosphorylated Stat3 (Stat3pY and Stat3pS) showed, however, no difference in Stat3 activation associated with inhibition of RhoA or Rac1 in DU145 cells (Figure 5A). Furthermore, suppression of Stat3 by adenoviral gene delivery of DNStat3 with WTStat3 or mock-infected cells as controls had no effect on total levels of Rho family GTPases Rac1, RhoA, and Cdc42 at 24, 48, or 72 hours after the adenoviral exposure (m.o.i. = 10) (Figure 5B).

In the next set of experiments, we tested whether Jak2 regulates Stat3 activation in human prostate cancer cells. DU145 cells were infected with adenovirus expressing DNJak2 with WTJak2 or mock-infected cells as the controls, and whole cell lysates were analyzed for Stat3 tyrosine phosphorylation by Western blotting at 24 and 48 hours after the adenoviral exposure at a m.o.i. of 10 (Figure 5C). Already at 24 hours, tyrosine phosphorylation of Stat3 was completely inhibited in cells expressing DNJak2, as detected by Western blotting, which suggested that Jak2 is critical for Stat3 activation in prostate cancer cells. Adenoviral gene delivery of WTJak2 increased Stat3 activation (Figure 5Ca). These findings prompted us to ask the question whether Jak2 also regulates the migration of DU145 cells. To test this in wound-filling assay, DU145 cells were infected with AdWTJak2, AdDNJak2, or AdLacZ at a m.o.i. of 10, and identical scratches were made in parallel wells. At 48 hours, migration of DU145 cells infected with adenovirus expressing WTJak2 was increased by 1.6-fold compared to cells expressing DNJak2 (Figure 5Cb). This was further confirmed by a modified Boyden chamber assay, which showed an ~2.5-fold increase in the number of migrated cells in the group infected with AdWTJak2- compared to AdDNJak2-infected cells ($P = 0.0003$) or AdLacZ-infected cells ($P < 0.0011$) (Figure 5Cc). When WTStat3 was introduced to DU145 cells simultaneously with WTJak2 using adenoviral gene delivery, WTJak2-induced migration of the cells in wound filling assay was increased twofold compared to the control group expressing WTJak2 and DNStat3 at the same m.o.i. (Figure 5Cd). These results suggested that the migration of DU145 cells induced by WTJak2 was suppressed by inhibition of Stat3. Finally, to examine whether Jak2 affects organization of the actin cytoskeleton in human prostate cancer cells, WTJak2 and DNJak2 were expressed using adenovirus in DU145 prostate cancer cells at a m.o.i. of 10. After 48 hours, the cells were fixed and immunostained for actin using FITC-conjugated secondary antibodies (Figure 5D). Similar to the effects of inhibition of Stat3, actin fibers were organized in an oval shape around the nuclei in prostate cancer cells expressing DNJak2, whereas adenoviral gene delivery of WTJak2 induced formation of actin stress fibers in the cell body as well as actin bundles extending to the filopodia (Figure 5D). In summary, the data gained from these studies suggested that Jak2 induces activation of Stat3 and the migratory phenotype of human prostate cancer cells.

Discussion

Disseminated prostate cancer is a significant challenge for clinical management of prostate cancer. The molecular mechanisms underlying metastatic spread of primary prostate cancer are unclear, therefore limiting the development of effective pharmacological therapies for advanced prostate cancer. In this work, we showed that transcription factor Stat3 induced a 33-fold increase in the number of lung metastases in an *in vivo* experimental prostate cancer metastases model. We further showed that Stat3 is constitutively active in 77% of lymph node and 67% of bone metastases of clinical prostate cancers. Stat3 induced motility of human prostate cancer cells in culture, and Jak2-activated Stat3 stimulated extension of cytoplasmic actin stress fibers and microtubules in pros-

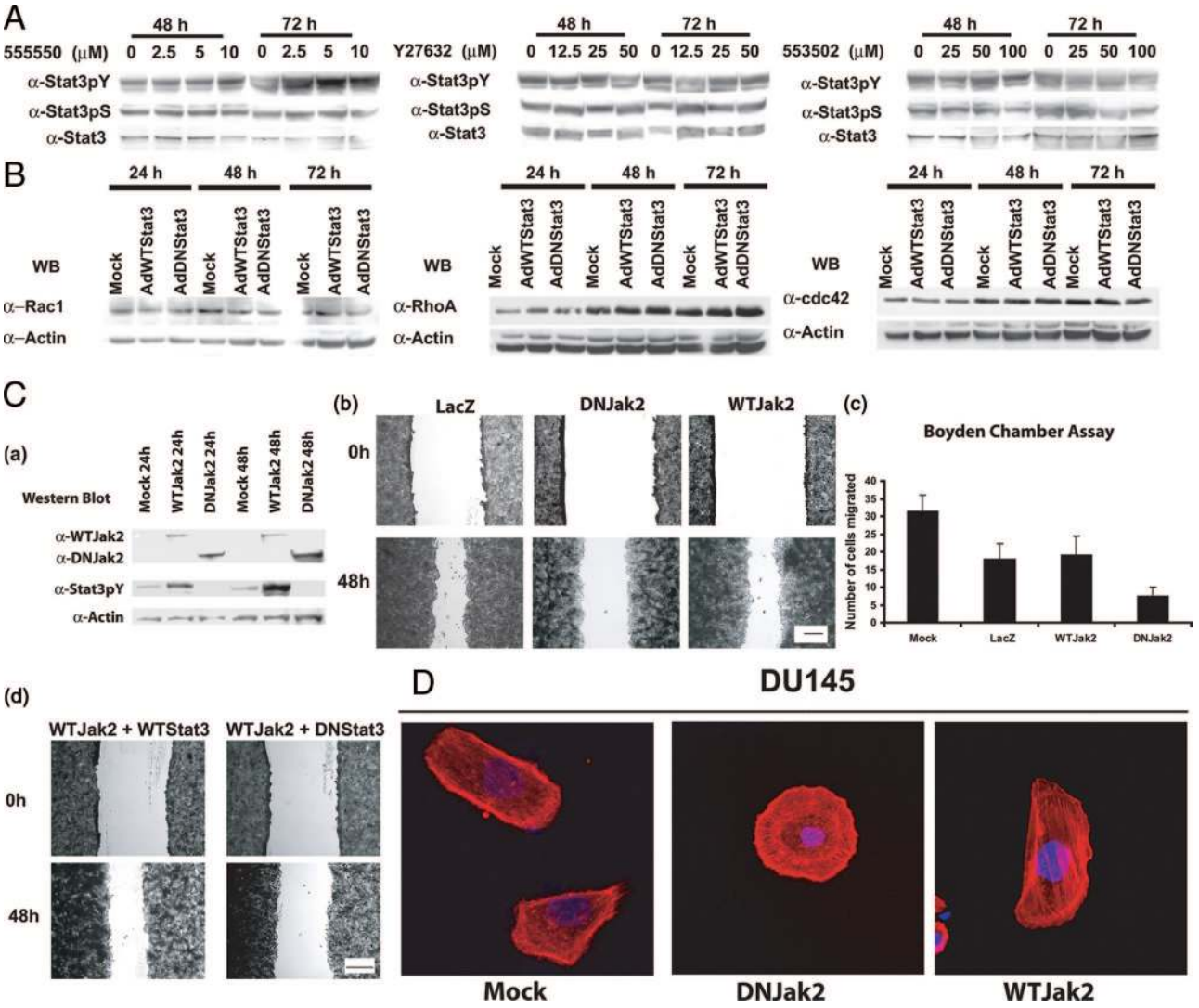

Figure 5. Jak2, but not RhoGTPases, contributes to the Stat3-induced migration of prostate cancer cells. **A:** DU145 cells were treated with pharmacological inhibitors of RhoA (555550 and Y27632) and Rac1 (553502) for 24, 48, and 72 hours at indicated concentrations. The levels of active forms of Stat3 (Stat3pY and Stat3pS) were analyzed by Western blotting from the whole cell lysates. Parallel samples were immunoblotted with anti-Stat3 mAb as indicated. **B:** Stat3 does not regulate Rac1, RhoA, or Cdc42 expression in DU145 cells. DU145 cells were infected with adenovirus expressing either WTStat3 or DNStat3 at a m.o.i. of 10. At 24, 48, and 72 hours after the adenoviral gene delivery, the levels of Rac1, RhoA, and Cdc42 protein expression were determined by Western blot analysis. The filters were stripped and reblotted with anti-actin pAb. **C:** Suppression of Jak2 inhibits phosphorylation of Stat3 and migration of DU145 cells. DU145 cells were infected with adenovirus expressing wild-type Jak2 (AdWTJak2) or dominant-negative Jak2 (AdDNJak2) at a m.o.i. of 10. **a:** The whole cell lysates were analyzed for Jak2 expression, tyrosine phosphorylation of Stat3, and for actin expression by Western blotting 24 and 48 hours after adenoviral gene delivery. To test the effect of Jak2 on prostate cancer cell migration, identical scratches were made in parallel wells of DU145 cells 24 hours after infection with AdWTJak2, AdDNJak2, or AdLacZ (m.o.i., 10) for 90 minutes. **b:** Photographs of the fixed cells (at 0, 24, 48, and 72 hours) after the adenoviral gene delivery were captured by phase contrast microscope (Nikon Eclipse TS100) equipped with a digital imaging system (Digital Sight DS-L1). Promotion of cell migration by WTJak2 was confirmed by modified Boyden chamber assays. DU145 cells were exposed to infection with adenovirus carrying either WTJak2, DNJak2, or LacZ at a m.o.i. of 10 for 90 minutes. **c:** Motility of DU145 cells through uncoated filters into the lower chamber of the microchemotaxis chambers filled with media containing 5% FBS was measured after 24 hours. Migrating cells were fixed, stained, and counted using phase contrast microscope in triplicate filters in three individual experiments (mean ± SD). To test whether Stat3 suppression will inhibit the cell migration induced by WTJak2, DU145 cells were infected with the combinations of adenoviral expressing WTJak2 and DNStat3 or WTJak2 and WTStat3 each at a m.o.i. of 5 for 90 minutes. Identical scratches were made in parallel wells and photographs of the fixed cells were captured by phase contrast microscope at 48 hours after the adenoviral gene delivery. **D:** Jak2 induces polarization of actin cytoskeleton in DU145 and PC-3 prostate cancer cells. DU145 and PC-3 cells grown on cover glasses were mock-infected or infected after 16 hours with a m.o.i. of 10 of AdWTJak2 or AdDNJak2 adenovirus. After 48 hours, the cells were fixed, permeabilized, and incubated with rhodamine-conjugated phalloidin using FITC-conjugated secondary antibodies. Cells were visualized and photographed under fluorescence microscopy (Zeiss LSM 510 imaging software). Representative images from one of three independent experiments are shown. Scale bars: 500 μm (**Cb**); 1000 μm (**Cd**).

tate cancer cells. These molecular changes likely underlie lamellipodia formation and the migratory phenotype of human prostate cancer cells induced by Stat3.

The key finding of this work is the robust Stat3 induction of lung metastases in an *in vivo* prostate cancer metastases model. This result is important because *in vitro* observations on invasiveness or motility of a cell line in culture do not necessarily translate into cells having the ability to metastasize *in vivo*. Previous reports have focused primarily on enhancement of prostate cancer cell growth by Stat3, which yielded somewhat conflicting results.[5,10,11,37–40] The work presented here is the first

study showing promotion of prostate cancer metastases by Stat3 *in vivo*. The experimental model in this work was tail-vein injections of nude mice with DU145 prostate cancer cells infected with adenovirus expressing wild-type Stat3 with LacZ or transcriptionally inactive Stat3 as controls. It is known that intravenous inoculation of cancer cells into tail veins of nude mice typically results in the development of metastases in the first capillary bed encountered. In this metastases assay, the first capillary network is in the lungs where the prostate cancer cell metastases developed. Future studies should focus on determining the Stat3-induced colonization patterns of human prostate cancer cells after inoculation of the cancer cells to the left cardiac ventricle. In addition, direct implantation of prostate cancer cells expressing active Stat3 into the long bones should determine whether Stat3 is involved in bone metastases formation of prostate cancer cells. Orthotopic prostate tumor growth studies would be able to address the question of whether Stat3 increases local invasion of prostate cancer cells to the neighboring tissues. Moreover, orthotopic prostate tumor growth studies will be able to establish whether human prostate cancer cells expressing active Stat3 will have increased capability to migrate to capillaries and lymphatic ducts in the primary tumor site.

Increased colonization of prostate cancer cells into lungs may reflect an increased ability of prostate cancer cells to survive in the pulmonary tissue environment when the cells overexpress active Stat3. An alternative explanation is that the increase in the number of lung metastases induced by Stat3 is attributable to increased extravasation of prostate cancer cells from the lung capillaries to the lung tissue. Enhanced extravasation of prostate cancer cells because of Stat3-stimulated cell motility is supported by our data obtained in cell culture. Specifically, Stat3 increased migration of human prostate cancer cells *in vitro* in both wound filling and Boyden chamber assays. We also found that Stat3 induced morphological changes characteristic of epithelial-to-mesenchymal transition of carcinoma cells such as lamellipodia formation and decreased cell clustering, which was consistent with the Stat3-induced motility of the cells. Lamellipodia formation of DU145 and PC-3 cells was accompanied by Stat3-induced changes in the actin cytoskeleton and the microtubule network. In the control cells, actin fibers and microtubules were arranged circularly around the nuclei, which is characteristic to nonmigratory cells. In contrast, in cells infected with adenovirus expressing WTStat3, actin fibers and microtubules extended toward the lamellipodia and the leading edge. The molecular mechanisms underlying Stat3-regulation of the microtubule network and rearrangement of actin fibers in human prostate cancer cells remain to be determined. Studies on potential Stat3 regulation of heterotypic adhesion of prostate cancer cells with endothelial cells are currently ongoing.

We showed in this work that Stat3 is constitutively active in the majority of prostate cancer metastases to lymph nodes and to bones. The factors and mechanisms contributing to the constitutive activation of Stat3 in human prostate cancer metastases are currently unclear. Such mechanisms may involve an autocrine loop of interleukin-6 in prostate cancer metastases. We show in this work that Jak2 activates Stat3 in prostate cancer cells. In contrast, inhibition of RhoGTPases, known to be involved in cell migration and known to activate Stat3 in several cell types,[18,19,35] had no effect on serine or tyrosine phosphorylation of Stat3 in prostate cancer cells. Activating mutations of Jak2 have been recently described in hematopoietic malignancies resulting in constitutive activation of Stat5.[41] Such Jak2 mutations may also occur in metastatic prostate cancer and result in constitutive activation of Stat3. A third potential mechanism for constitutive activation of Stat3 in prostate cancer metastases is amplification of the Stat3 gene. This is particularly interesting because the gene encoding Stat3 is located in chromosome 17,[32] which is frequently altered in prostate cancer.[42]

In conclusion, this work provides the first evidence of involvement of transcription factor Stat3 in prostate cancer metastases *in vivo*. Studies testing newly developed pharmacological inhibitors of Stat3[43–45] in prostate cancer should include testing their efficacy in inhibiting metastatic spread of prostate cancer in experimental metastases models of prostate cancer *in vivo*.

Acknowledgments

We thank Drs. Shyh-Han Tan and Zhiyong Liao for providing critical feedback for this manuscript; and Dr. Hallgeir Rui for AdLacZ, AdDNStat3, AdWTStat3, AdWTJak2, and AdDNJak2 constructs.

References

1. Arya M, Bott SR, Shergill IS, Ahmed HU, Williamson M, Patel HR: The metastatic cascade in prostate cancer. Surg Oncol 2006, 15:117–128
2. Ihle JN: The Stat family in cytokine signaling. Curr Opin Cell Biol 2001, 13:211–217
3. Levy DE, Darnell Jr JE: Stats: transcriptional control and biological impact. Nat Rev Mol Cell Biol 2002, 3:651–662
4. Wen Z, Zhong Z, Darnell Jr JE: Maximal activation of transcription by Stat1 and Stat3 requires both tyrosine and serine phosphorylation. Cell 1995, 82:241–250
5. Mora LB, Buettner R, Seigne J, Diaz J, Ahmad N, Garcia R, Bowman T, Falcone R, Fairclough R, Cantor A, Muro-Cacho C, Livingston S, Karras J, Pow-Sang J, Jove R: Constitutive activation of Stat3 in human prostate tumors and cell lines: direct inhibition of Stat3 signaling induces apoptosis of prostate cancer cells. Cancer Res 2002, 62:6659–6666
6. Campbell CL, Jiang Z, Savarese DM, Savarese TM: Increased expression of the interleukin-11 receptor and evidence of STAT3 activation in prostate carcinoma. Am J Pathol 2001, 158:25–32
7. Huang HF, Murphy TF, Shu P, Barton AB, Barton BE: Stable expression of constitutively-activated STAT3 in benign prostatic epithelial cells changes their phenotype to that resembling malignant cells. Mol Cancer 2005, 4:2–8
8. Dhir R, Ni Z, Lou W, DeMiguel F, Grandis JR, Gao AC: Stat3 activation in prostatic carcinomas. Prostate 2002, 51:241–246
9. Horinaga M, Okita H, Nakashima J, Kanao K, Sakamoto M, Murai M: Clinical and pathologic significance of activation of signal transducer and activator of transcription 3 in prostate cancer. Urology 2005, 66:671–675
10. Lee SO, Lou W, Hou M, de Miguel F, Gerber L, Gao AC: Interleukin-6 promotes androgen-independent growth in LNCaP human prostate cancer cells. Clin Cancer Res 2003, 9:370–376
11. Barton BE, Karras JG, Murphy TF, Barton A, Huang H: Signal trans-

ducer and activator of transcription (STAT3) activation in prostate cancer: direct STAT3 inhibition induces apoptosis in prostate cancer lines. Mol Cancer Ther 2004, 3:11–20
12. Dauer DJ, Ferraro B, Song L, Yu B, Mora L, Buettner R, Enkemann S, Jove R, Haura EB: Stat3 regulates genes common to both wound healing and cancer. Oncogene 2005, 24:3397–3408
13. Xie TX, Huang FJ, Aldape KD, Kang SH, Liu M, Gershenwald JE, Xie K, Sawaya R, Huang S: Activation of stat3 in human melanoma promotes brain metastasis. Cancer Res 2006, 66:3188–3196
14. Li WC, Ye SL, Sun RX, Liu YK, Tang ZY, Kim Y, Karras JG, Zhang H: Inhibition of growth and metastasis of human hepatocellular carcinoma by antisense oligonucleotide targeting signal transducer and activator of transcription 3. Clin Cancer Res 2006, 12:7140–7148
15. Silver DL, Naora H, Liu J, Cheng W, Montell DJ: Activated signal transducer and activator of transcription (STAT) 3: localization in focal adhesions and function in ovarian cancer cell motility. Cancer Res 2004, 64:3550–3558
16. Horiguchi A, Oya M, Shimada T, Uchida A, Marumo K, Murai M: Activation of signal transducer and activator of transcription 3 in renal cell carcinoma: a study of incidence and its association with pathological features and clinical outcome. J Urol 2002, 168:762–765
17. Kusaba T, Nakayama T, Yamazumi K, Yakata Y, Yoshizaki A, Nagayasu T, Sekine I: Expression of p-STAT3 in human colorectal adenocarcinoma and adenoma; correlation with clinicopathological factors. J Clin Pathol 2005, 58:833–838
18. Aznar S, Valeron PF, del Rincon SV, Perez LF, Perona R, Lacal JC: Simultaneous tyrosine and serine phosphorylation of STAT3 transcription factor is involved in Rho A GTPase oncogenic transformation. Mol Biol Cell 2001, 12:3282–3294
19. Debidda M, Wang L, Zang H, Poli V, Zheng Y: A role of STAT3 in Rho GTPase-regulated cell migration and proliferation. J Biol Chem 2005, 280:17275–17285
20. Faruqi TR, Gomez D, Bustelo XR, Bar-Sagi D, Reich NC: Rac1 mediates STAT3 activation by autocrine IL-6. Proc Natl Acad Sci USA 2001, 98:9014–9019
21. Pelletier S, Duhamel F, Coulombe P, Popoff MR, Meloche S: Rho family GTPases are required for activation of Jak/STAT signaling by G protein-coupled receptors. Mol Cell Biol 2003, 23:1316–1333
22. Hall A: Rho GTPases and the actin cytoskeleton. Science 1998, 279:509–514
23. Ng DC, Lin BH, Lim CP, Huang G, Zhang T, Poli V, Cao X: Stat3 regulates microtubules by antagonizing the depolymerization activity of stathmin. J Cell Biol 2006, 172:245–257
24. Saramäki O, Willi N, Bratt O, Gasser TC, Koivisto P, Nupponen NN, Bubendorf L, Visakorpi T: Amplification of EIF3S3 gene is associated with advanced stage in prostate cancer. Am J Pathol 2001, 159:2089–2094
25. Zellweger T, Ninck C, Bloch M, Mirlacher M, Koivisto PA, Helin HJ, Mihatsch MJ, Gasser TC, Bubendorf L: Expression patterns of potential therapeutic targets in prostate cancer. Int J Cancer 2005, 113:619–628
26. Sultan AS, Xie J, LeBaron MJ, Ealley EL, Nevalainen MT, Rui H: Stat5 promotes homotypic adhesion and inhibits invasive characteristics of human breast cancer cells. Oncogene 2005, 24:746–760
27. Nemeth JA, Harb JF, Barroso Jr U, He Z, Grignon DJ, Cher ML: Severe combined immunodeficient-hu model of human prostate cancer metastasis to human bone. Cancer Res 1999, 59:1987–1993
28. Timár J, Raso E, Dome B, Li L, Grignon D, Nie D, Honn KV, Hagmann W: Expression, subcellular localization and putative function of platelet-type 12-lipoxygenase in human prostate cancer cell lines of different metastatic potential. Int J Cancer 2000, 87:37–43
29. Pulukuri SM, Gondi CS, Lakka SS, Jutla A, Estes N, Gujrati M, Rao JS: RNA interference-directed knockdown of urokinase plasminogen activator and urokinase plasminogen activator receptor inhibits prostate cancer cell invasion, survival, and tumorigenicity in vivo. J Biol Chem 2005, 280:36529–36540
30. Muramaki M, Miyake H, Hara I, Kamidono S: Synergistic inhibition of tumor growth and metastasis by combined treatment with TNP-470 and docetaxel in a human prostate cancer PC-3 model. Int J Oncol 2005, 26:623–628
31. Knox JD, Mack CF, Powell WC, Bowden GT, Nagle RB: Prostate tumor cell invasion: a comparison of orthotopic and ectopic models. Invasion Metastasis 1993, 13:325–331
32. Clark J, Edwards S, Feber A, Flohr P, John M, Giddings I, Crossland S, Stratton MR, Wooster R, Campbell C, Cooper CS: Genome-wide screening for complete genetic loss in prostate cancer by comparative hybridization onto cDNA microarrays. Oncogene 2003, 22:1247–1252
33. Yamazaki D, Kurisu S, Takenawa T: Regulation of cancer cell motility through actin reorganization. Cancer Sci 2005, 96:379–386
34. Etienne-Manneville S: Actin and microtubules in cell motility: which one is in control? Traffic 2004, 5:470–477
35. Simon AR, Vikis HG, Stewart S, Fanburg BL, Cochran BH, Guan KL: Regulation of STAT3 by direct binding to the Rac1 GTPase. Science 2000, 290:144–147
36. Jaffe AB, Hall A: Rho GTPases: biochemistry and biology. Annu Rev Cell Dev Biol 2005, 21:247–269
37. Spiotto MT, Chung TD: STAT3 mediates IL-6-induced growth inhibition in the human prostate cancer cell line LNCaP. Prostate 2000, 42:88–98
38. Spiotto MT, Chung TD: STAT3 mediates IL-6-induced neuroendocrine differentiation in prostate cancer cells. Prostate 2000, 42:186–195
39. Steiner MS: Role of peptide growth factors in the prostate: a review. Urology 1993, 42:99–110
40. Godoy-Tundidor S, Cavarretta IT, Fuchs D, Fiechtl M, Steiner H, Friedbichler K, Bartsch G, Hobisch A, Culig Z: Interleukin-6 and oncostatin M stimulation of proliferation of prostate cancer 22Rv1 cells through the signaling pathways of p38 mitogen-activated protein kinase and phosphatidylinositol 3-kinase. Prostate 2005, 64:209–216
41. Baxter EJ, Scott LM, Campbell PJ, East C, Fourouclas N, Swanton S, Vassiliou GS, Bench AJ, Boyd EM, Curtin N, Scott MA, Erber WN, Green AR: Acquired mutation of the tyrosine kinase JAK2 in human myeloproliferative disorders. Lancet 2005, 365:1054–1061
42. Gillanders EM, Xu J, Chang BL, Lange EM, Wiklund F, Bailey-Wilson JE, Baffoe-Bonnie A, Jones M, Gildea D, Riedesel E, Albertus J, Isaacs SD, Wiley KE, Mohai CE, Matikainen MP, Tammela TL, Zheng SL, Brown WM, Rokman A, Carpten JD, Meyers DA, Walsh PC, Schleutker J, Gronberg H, Cooney KA, Isaacs WB, Trent JM: Combined genome-wide scan for prostate cancer susceptibility genes. J Natl Cancer Inst 2004, 96:1240–1247
43. Jing N, Sha W, Li Y, Xiong W, Tweardy DJ: Rational drug design of G-quartet DNA as anti-cancer agents. Curr Pharm Des 2005, 11:2841–2854
44. Turkson J, Kim JS, Zhang S, Yuan J, Huang M, Glenn M, Haura E, Sebti S, Hamilton AD, Jove R: Novel peptidomimetic inhibitors of signal transducer and activator of transcription 3 dimerization and biological activity. Mol Cancer Ther 2004, 3:261–269
45. Song H, Wang R, Wang S, Lin J: A low-molecular-weight compound discovered through virtual database screening inhibits Stat3 function in breast cancer cells. Proc Natl Acad Sci USA 2005, 102:4700–4705 ;